On the influence of a swirling motion on the wake of a porous disc: an experimental investigation

Ernesto Fuentes Noriega, Cédric Raibaudo, Régine Weber, Nicolas Mazellier

On the influence of a swirling motion on the wake of a porous disc: an experimental investigation

E. FUENTES NORIEGA[a], C. RAIBAUDO[a], R. WEBER[a]
N. MAZELLIER[a]

a. University of Orléans, INSA-CVL, PRISME, EA 4229, 45072 Orléans, France
ernesto.fuentes-noriega@univ-orleans.fr (corresponding author)

Résumé :

Ce travail expérimental porte sur l'étude du sillage d'un disque poreux non-uniforme en modifiant le calage de pales. L'objectif de cette modification est d'introduire une composante azimuthale de la vitesse, actuellement absente dans les études sur disques poreux, afin de représenter plus fidèlement les caractéristiques des sillages éoliens. Pour quantifier l'impact des modifications apportées, des essais en soufflerie ont été effectués à partir de mesures d'anémométrie fil-chaud 3-Composantes couplées à des mesures PIV et à des mesures de forces aérodynamique. Les résultats montrent qu'en ajoutant un calage de pales de 15°, le coefficient de trainée C_D reste inchangé et les vitesses azimuthales obtenues sont de l'ordre de 15% *de la vitesse de l'écoulement incident. Les résultats montrent aussi que le sillage du disque poreux modifié se caractérise par des profils de déficit de vitesse de forme Gaussienne et autosimilaires qui s'accordent de manière plus fidèle avec les profils rapportés dans la littérature (mesures expérimentales et simulations numériques d'éoliennes à échelle réduite et à échelle réelle.)*

Abstract :

This study presents the results of an experimental investigation of a modified non-uniform porous disc wake with pitched blades. These modifications introduce an azimuthal velocity component characteristic of wind turbine wakes and currently absent in the case of porous discs found in the current scientific literature. In order to characterize the influence of the modifications on the wake, an experimental wind-tunnel study was carried out using 3-component hot-wire anemometry measurements (HWA) coupled with planar PIV measurements and force measurements using an aerodynamic balance. The results show that, by adding a constant pitch of 15°, the drag coefficient C_D remains unchanged and the azimuthal velocities obtained are of the order of 15% *of the free-stream velocity. The results also show that the swirling wake has Gaussian-shaped self-similar velocity deficit profiles which are more in agreement with the velocity profiles found in the literature (experimental measurements and numerical simulations of lab-scale and real-sized wind turbines).*

Key Words : wake, porous disc, swirl, wind turbine, self-similarity

1 Introduction

Porous discs have been frequently used as a surrogate for modeling the wake of a wind turbine over the last decades. Currently, the design of porous discs is mainly based on the choice of the porosity of the disc, which is adjusted so that the drag coefficient C_D of the disc matches the thrust coefficient C_T of the wind turbine. While homogeneous porosity has been extensively used in literature [1] [2] [3], more recently porous discs based on non-homogeneous porosity have been studied [4] [5] [6] . These studies emphasized that the main features of the mean wake of the porous disc (e.g., velocity deficit, Reynolds stresses ...) compare fairly well to those of the wake of the wind turbine, at least far enough from the obstacle. However, the near wake differs noticeably from flow to flow. One of the key parameters missing in the near wake of the porous disc is the angular momentum provided by the swirl velocity, which is induced by the blade motion [4] . Since the near wake represents the initial conditions of the far wake, it is fundamental to reproduce the characteristics of the near wake to faithfully mimic the wake of the wind turbine.

In this study, this issue is tackled by investigating the wake of a modified porous disc compared to that proposed in [5]. This modified porous disc incorporates a swirling effect in the wake by pitching the blades of the non-uniform porous disc of an angle α. The discs were 3D printed using polylactic acid (PLA) and the pitch angle was varied from 5° to 30°. In order to investigate the influence of the swirl on the wake properties, wind-tunnel experiments were conducted over a wide range of operating conditions. Force measurements using an aerodynamic balance, coupled with planar Particle Image Velocimetry (PIV2D2C) and 3-components hot wire anemometry (3C-HWA) were performed to analyze the wake structure for the most relevant porous discs.

This study aims at characterizing the wake of the modified porous disc with the swirling effect. Particular attention is given to the shape of the velocity deficit with a self-similar scaling [7]. The experimental set-up and experiment details are presented in §2, the results and discussions are explained in §3 and conclusions and implications are given at the end of this article.

2 Experimental set up

2.1 Wind tunnel and test rig

Experiments were conducted in the S2 open-circuit wind tunnel of the PRISME Laboratory at the University of Orléans. The test section is 2 m long with a cross-sectional area of 0.50 m $\times$ 0.50 m. The diameter and the thickness of the non-uniform porous discs used in this experiment are D = 100 mm and e = 5 mm respectively. The discs were mounted to an ATI Mini40-E aerodynamic force balance placed directly below the wind tunnel floor with a T-shaped aluminum rod with a diameter of d = 6mm. The resulting wind tunnel blockage ratio is approximately 2% (rod included) ensuring an undisturbed wake expansion. The test rig was subjected to a uniform inflow of $U_\infty = 20m.s^{-1}$, corresponding to a Reynolds number of $Re_D = U_\infty D/\nu$ of 10^5 (ν is the kinematic viscosity of air) with a background turbulence intensity of around 0.3%.

The results for two main porous discs are presented in this study: the reference porous disc NHD35 (case A) used in [5] (Non-Homogeneous Holes Disc with 35% Solidity) and a modified NHD35 porous disc with 15° of pitch angle NHD35-s15 (case B).

2.2 Measurement techniques

The following results were obtained using a combination of 3-components hot-wire anemometry and planar particle image velocimetry measurements. The HWA measurements were performed using a Dantec Streamline constant temperature anemometry (CTA) system with a Platinum-plated tungsten tri-axial wire probe (Dantec Dynamics 55P91 probe). The probe has a wire diameter of $5\mu m$, an individual wire sensing length of 1.2 mm and a total sensing length of 3 mm. For the HWA experiments, cross-sectional YZ planes (see Fig. 1) were mapped at $X = 2D$ (near wake) and at $X = 6D$ (far wake). Between 2D and 6D, vertical and horizontal profiles were measured every 0.5D.

For the PIV2D2C measurements, 3 planes were explored from $X = -2D$ to $X = 8D$ in order to capture the full development of the wake. An overlapping area of $1D$ (i.e 25%) was ensured between each plane. The size of the individual fields of view (FOV) were 420 mm (4.2D) $\times$ 260 mm (2.6D) and the total monitored area equaled 1000 mm (10D) $\times$ 260 mm (2.6D) as shown in Figs. 1 & 3. The image sets were captured using a commercial 11 megapixels La Vision LX-11 camera equipped with an 85 mm ZEISS lens. The illumination was provided by a two-pulse Nd:YAG laser system (La Vision, Twins BSL) which generated a green (532 nm) laser sheet. The laser and the camera were mounted on rails parallel to the test section. The experiments performed during this campaign are summarized in Figure 1 along with the coordinate system and the origin.

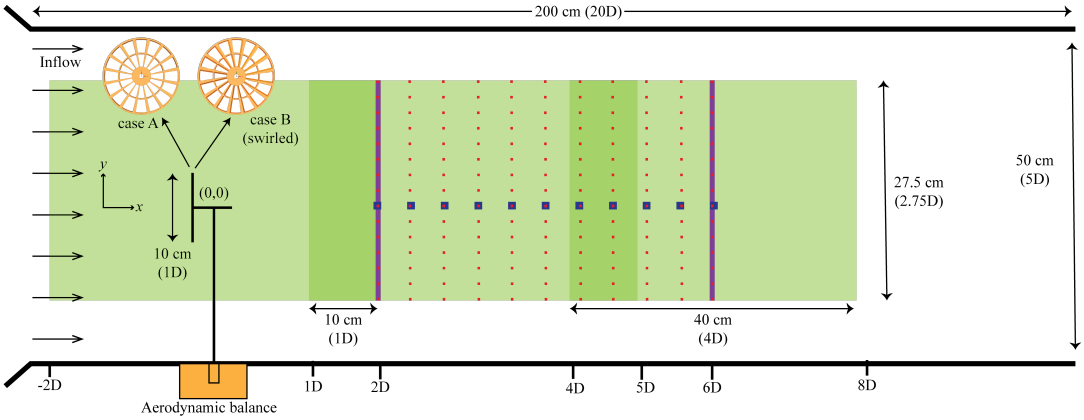

Figure 1: Side view drawing of the wind tunnel experimental set-up (not to scale). Green boxes represent the 2D2C PIV measurements regions, the magenta solid lines represent the cross-sectional YZ 3C-HWA mapped planes, the dotted red lines represent the 3C-HWA vertical profiles and the blue squares represent the 3C-HWA horizontal profiles (out of plane) measurements. D is the diameter of the Discs.

Force balance measurements were conducted in order to directly calculate the drag coefficients C_D (see Eq. 1) of the porous discs.

$$C_D = \frac{F_D}{\frac{1}{2}\rho_{air} A U_\infty^2} \tag{1}$$

Where F_D is the measured drag force of the porous disc, ρ_{air} is the density of air and $A = \pi(D/2)^2$ is the chosen reference area. The drag coefficients values reached an asymptote for large values of Reynolds ($Re \geq 10^4$) corroborating the findings in [5].

These results show that the modifications added to the NHD35 disc (case A) did not significantly change the value of the drag coefficient $C_D = 0.56 \pm 0.03$ for case A and $C_D = 0.57 \pm 0.03$ for case B. As both

porous discs have the same diameter and drag coefficient, according to the current design procedure for porous discs as wind turbine surrogates, these two discs are equivalent. The question which is addressed in the following, relies on the wake structure.

3 Results & discussions

3.1 Swirling motion in the wake

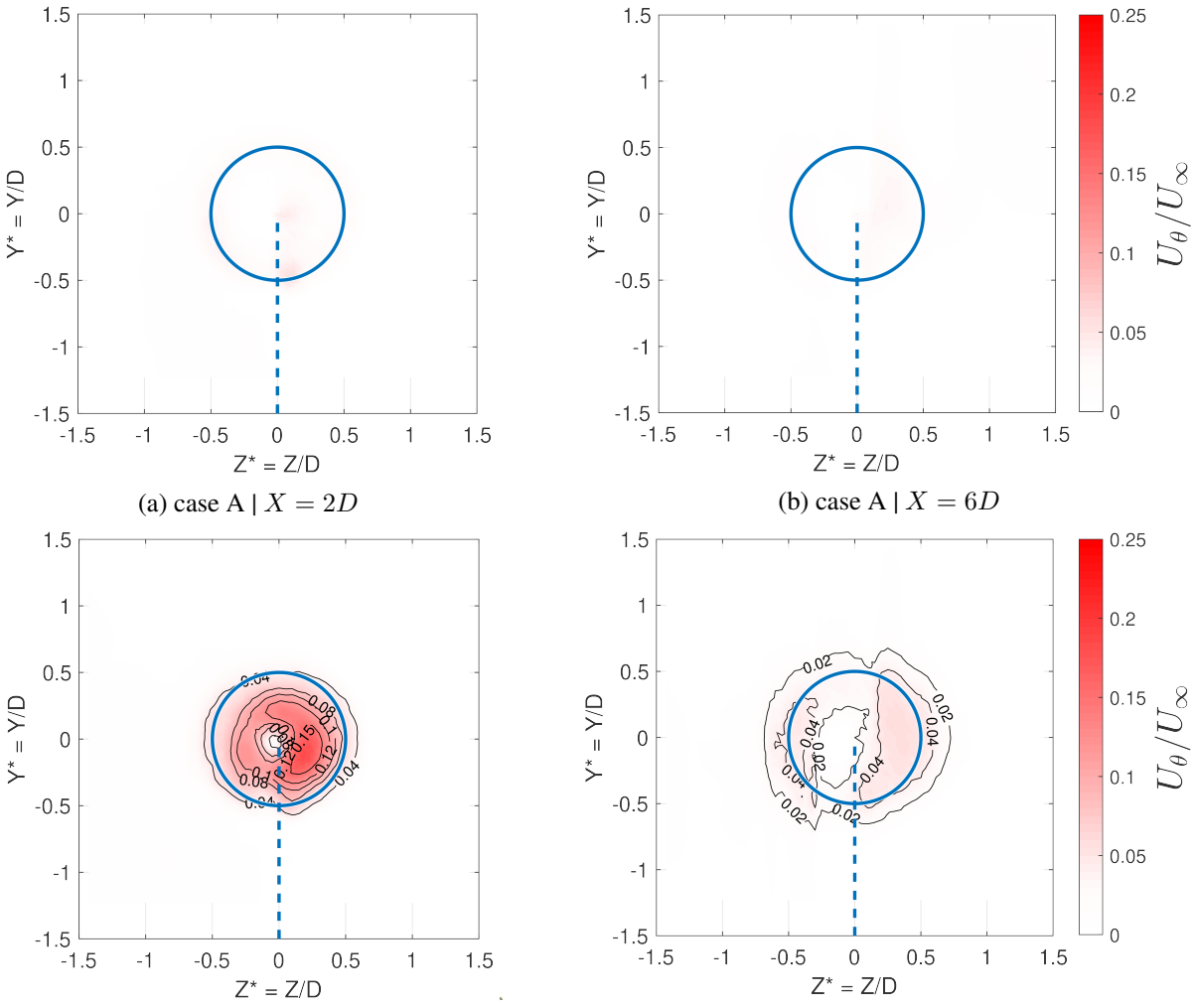

(a) case A | $X = 2D$

(b) case A | $X = 6D$

(c) case B | $X = 2D$

(d) case B | $X = 6D$

Figure 2: Azimuthal velocity U_θ maps (3C-HWA) normalized by the free stream velocity U_∞ for case A (top line) and case B (bottom line) evaluated at $X = 2D$ (left) and at $X = 6D$ (right). The solid blue line represents the contour of the porous disc and the dashed blue line represents the cylindrical rod. The spatial resolution of the measurements is 5 mm.

In the remainder of this article, unless specified otherwise, all physical variables are presented in dimensionless form using the porous disc diameter D and the free-stream velocity U_∞ as scaling parameters. Figure 2 shows the normalized azimuthal velocity U_θ calculated with the time averaged values of the vertical velocity component $\overline{V}$ and of the spanwise velocity component $\overline{W}$ measured with the 3C-HWA. (see Eq. 2).

$$U_\theta = \overline{W} sin(\theta) - \overline{V} cos(\theta) \tag{2}$$

The reference porous disc NHD35 (case A) has no azimuthal velocity in the wake [4]. The modified porous disc (Case B) shows that by pitching the blades of the NHD35 disc [5], an azimuthal component U_θ of the velocity is introduced in the wake. This component reaches values of up to 15% of the free stream velocity U_∞ at $X = 2D$ and 4% at $X = 6D$. The swirling area spreads radially as the wake expansions takes place downwind of the test rig. The asymmetrical distribution of the azimuthal velocity field can be due to the wake of the mast breaking the axissymmetrical nature of the porous disc wake.

The modifications added to the porous disc resulted in a swirling wake with an azimuthal component which is characteristic of a wind turbine wake.

3.2 Velocity deficit and self-similarity

Figure 3 shows the resulting normalized mean streamwise velocity field $\overline{U}(x, y)$ for case A (top) and case B (bottom). The black solid lines represent the normalized vertical velocity profiles at different downwind locations. The velocity profiles for the reference case A shows two velocity minima located around the edges of the porous disc (white dashed lines) where the strongest shear is produced, with a slight velocity overshoot area in between. This dip fades and the peaks are smoothed as the wake develops. At around $X = 6D$, the peaks are no longer noticeable and the velocity profiles present a bell curve shape.

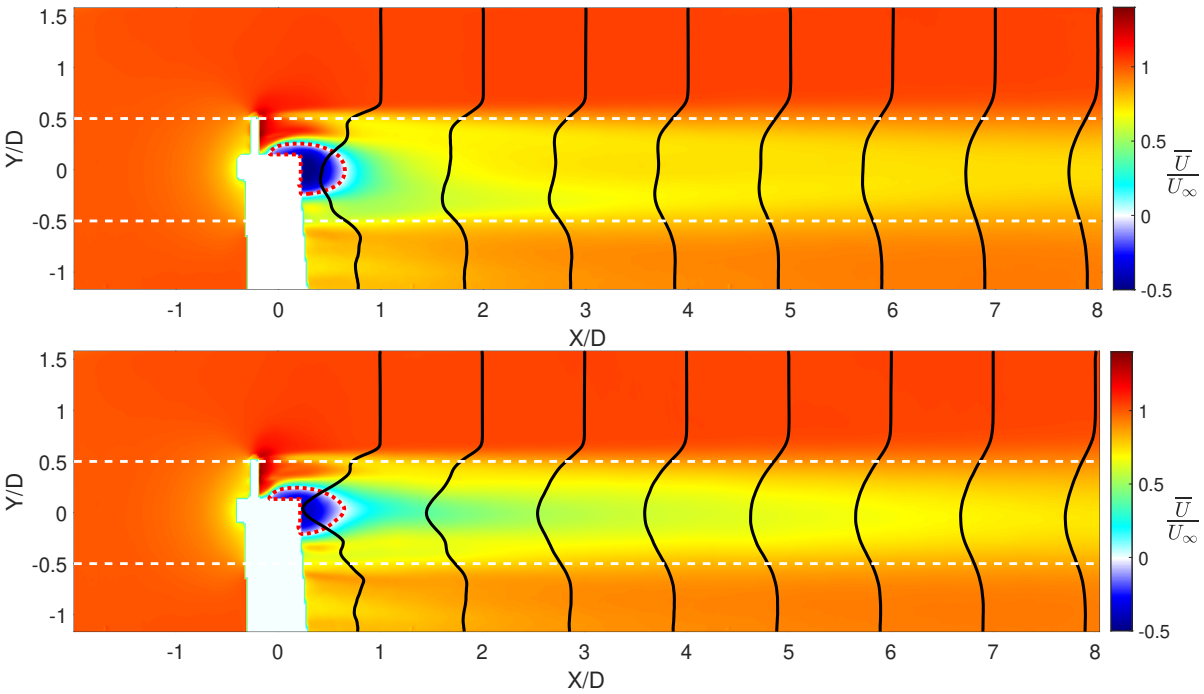

Figure 3: Average streamwise velocity fields (PIV) normalized by the free-stream velocity U_∞ for case A (Top) and case B (bottom). The white area near $X = 0D$ is the masked zone where the test rig is located. The dashed white lines represent the edges of the porous disc. The black lines represent the mean streamwise velocity profile evolution along the wake and the red dashed line represents the $\overline{U} = 0$ iso-contour.

On the other hand, the disc with the swirling wake (case B) shows velocity profiles that become Gaussian (see Figs. 4 & 5) much quicker ($X = 3D$). This Gaussian shape has been observed in many wind tunnel experiments using lab-scale wind turbines[3] [9] [14] , numerical simulations [15] [16] and in data of operating wind farms [12]. These observations were also the basis for the development of the new analytical model proposed in [12] and presented in [13] to predict the deficit of the streamwise velocity in the wake of wind turbines.

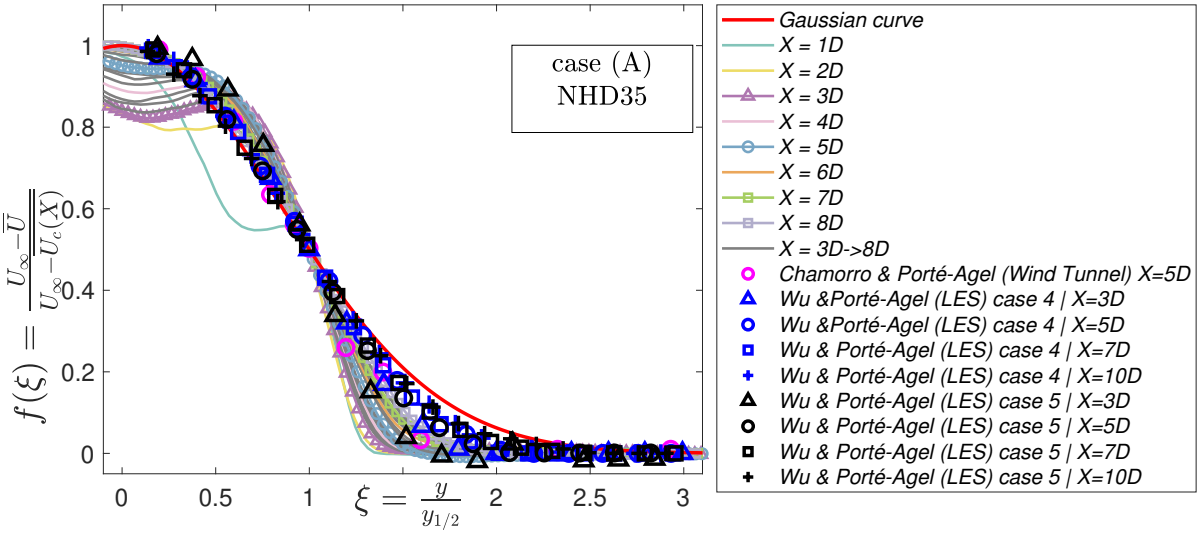

(a)

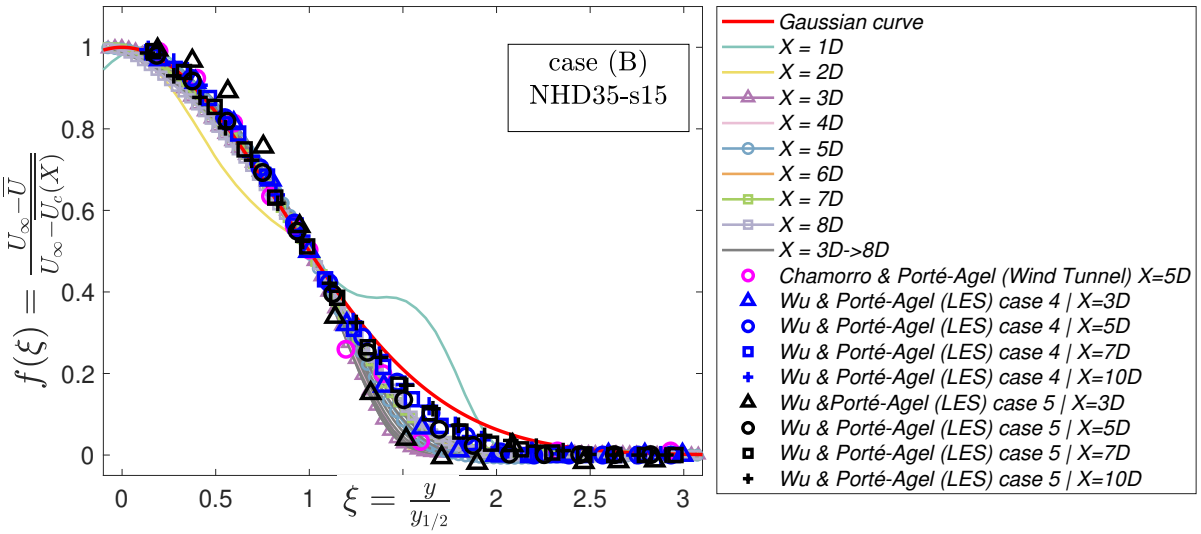

(b)

Figure 4: Self-similar velocity deficit top-half profiles of the wind-tunnel PIV2D2C measurements for (a) case A [5] and (b) case B. The pink circles correspond to the lab-scale 3-bladed wind turbine experiments studied in [14]. The other data points correspond to the LES performed in [15] of a Vestas V80-2MW wind turbine. Case 4 has a terrain roughness of $z_0 = 0.005$ m and of $z_0 = 0.00005$ m for case 5.

Figure 3 also shows that the wake of the aluminum rod holding the porous disc creates a shear zone distinguishable up until $X = 3D - 4D$. The wake generated by the cylindrical rod breaks the symmetry of the velocity profiles for both cases. Nevertheless, it could be noted that for the non-swirled wake (case A) the center of the wake, i.e where the velocity is at its minimum, is downwashed. This is not the case

for the swirled wake (case B) as it resists better to the downwash and remains fairly centered.

A Gaussian shaped velocity deficit profile is characteristic of the far wake of a bluff body [7] and is associated with a self-similar behavior. If the velocity deficit $\Delta U = U_\infty - \overline{U}$ is scaled by the maximum velocity deficit $\Delta U_{max} = U_\infty - U_c(X)$ (where $U_c(X)$ is the minimum velocity at X) and the distances are scaled by the wake half-width $y_{\frac{1}{2}}$, the self-similar velocity deficit evolution can be evaluated for each porous disc. Figure 4 shows the self-similar top-half velocity deficit vertical profiles of the PIV measurements. Figure 5 shows the velocity deficit full horizontal profiles of the HWA measurements. The latter profiles are more symmetric because horizontal profiles are less affected by the symmetry break produced by the cylindrical rod.

The results show that the swirled wake becomes self-similar after 3 disc diameters and the profiles collapse fairly well with the wind tunnel and numerical simulations found in the literature [12] - [15]. In contrast, the reference case A, has a top-hat shape up until approximately 6 disc diameters where it starts to become Gaussian. This hints at the possibility that one of the main mechanisms behind self-similarity in the wakes of wind turbines is the swirling aspect of the wake.

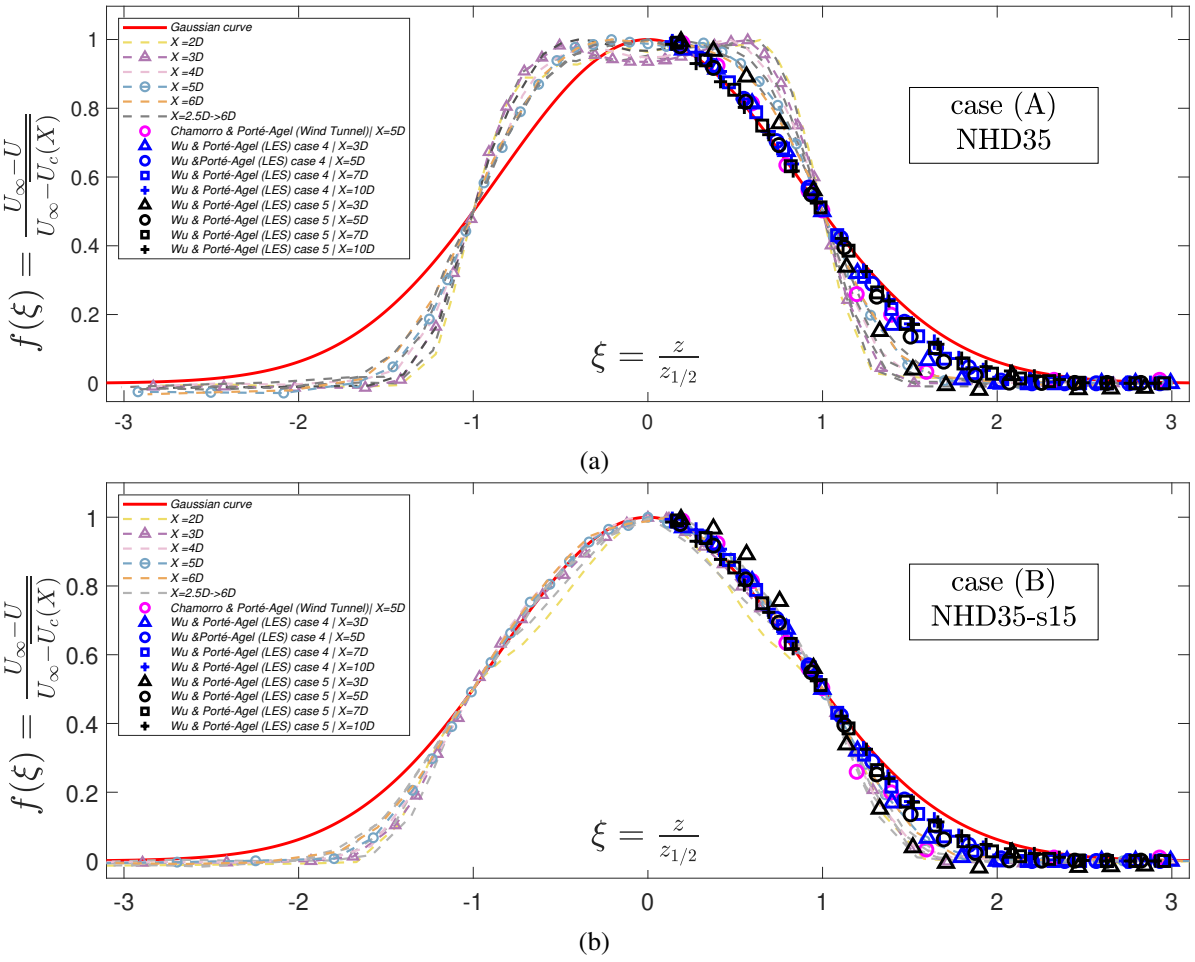

Figure 5: Self-similar horizontal velocity deficit profiles of the wind-tunnel HWA measurements for (a) case A [5] and (b) case B.

Conclusion

This experimental investigation presents the results of the wind tunnel study of the turbulent wake of a modified non-uniform porous disc. The modifications brought to the non-uniform disc NHD35 [5] aimed at introducing a swirling motion to the wake through the addition of a constant pitch angle to the disc blades. Force measurements using an aerodynamic balance, coupled with planar particle image velocimetry and 3-components hot wire anemometry were performed to analyze the wake structure. The pitch angle $\alpha = 15°$ generated azimuthal velocities of up to 15% of the external velocity U_∞ in the near wake and of 4% in the far wake without increasing the value of the drag coefficient C_D despite the slight increase of the projected blocked area.

PIV and HWA measurements show that the swirling motion in the turbulent wake speeds up self-similarity and the velocity profiles become Gaussian in shape at $X = 3D$ as opposed to $X = 6D$ for the non-swirled wake. A self-similar Gaussian shape for the velocity deficit function has been widely observed in the literature for wind tunnel experiments using lab-scale wind turbines, LES of real size wind turbines as well as in wind farms field LIDAR measurements. The velocity deficit profiles of the swirled wake collapse better with these results and with the Gaussian model proposed in [12].

All in all, these results show that the pitch is an interesting and inexpensive parameter to introduce to porous discs as surrogates for wind turbine wakes. The wake contains the swirling motion missing from classical porous disc wakes [4] and present self-similar Gaussian velocity deficit profiles with striking resemblance to the results found in the literature.

Further investigations will be carried out in order to shed light on the mechanisms that speed up self-similarity in regards of the introduced swirling motion. Moreover, a characterization of the turbulence will complete the investigation of the modifications brought to the porous disc wake.

References

[1] Aubrun S., Wind turbine wake properties : Comparison between a non-rotating simplified wind turbine model and a rotating model, Journal of Wind Engineering and Industrial Aerodynamics, 2013.

[2] Aubrun, S., Bastankhah, M., Cal, et al., Round-Robin Tests of Porous Disc Models, Phys.: Conf. Ser., 1256, p. 012004. 2019.

[3] Lignarolo LEM, Ragni D, Ferreira CJ, Experimental comparison of a wind-turbine and of an actuator-disc near wake, Journal of Renewable Sustainable Energy, 2016.

[4] Camp EH, Cal RB., Mean kinetic energy transport and event classification in a model wind turbine array versus an array of porous disks: Energy budget and octant analysis., Phys Rev Fluids. 1(4):044404. 2016.

[5] Helvig S de J, Vinnes MK, Segalini A, Worth NA, Hearst RJ, A comparison of lab-scale free rotating wind turbines and actuator disks, Journal of Wind Engineering and Industrial Aerodynamics, 2021.

[6] Howland MF, Bossuyt J, Martínez-Tossas LA, Meyers J, Meneveau C., Wake structure in actuator disk models of wind turbines in yaw under uniform inflow conditions, Journal of Renewable Sustainable Energy, 8(4):043301. 2016.

[7] Pope S., Turbulent Flows Cambridge University Press, p147-160 2000.

[8] Travis KN, Smith SE, Vignal L, Djeridi H, Bourgoin M, Cal RB, et al., Characterization of coupling between inertial particles and turbulent wakes from porous disk generators, Journal of Fluid Mechanics, 933:A42. 2022.

[9] Stevens RJAM, Meneveau C., Flow Structure and Turbulence in Wind Farms, Annual Review of Fluid Mechanics, 49(1):311–39. 2017.

[10] Jensen NO., A note on wind generator interaction, Risø National Laboratorys, Roskilde, Denmark, 1983.

[11] Frandsen S, Barthelmie R, Pryor S, Rathmann O, Larsen S, Højstrup J, et al., Analytical modelling of wind speed deficit in large offshore wind farms, Wind Energy, 9(1–2):39–53. 2006.

[12] Bastankhah, M., Porté-Agel, F., A New Analytical Model for Wind-Turbine Wakes, Renewable Energy, 70, pp. 116–123, 2014.

[13] Porté-Agel, F., Wind-Turbine and Wind-Farm Flows: A Review, Springer, p. 59., 2019.

[14] Chamorro LP, Porté-Agel F., Effects of Thermal Stability and Incoming Boundary-Layer Flow Characteristics on Wind-Turbine Wakes: A Wind-Tunnel Study, Boundary-Layer Meteorology, 136(3):515–33. 2010.

[15] Wu YT, Porté-Agel F., Atmospheric Turbulence Effects on Wind-Turbine Wakes: An LES Study, Energies, 5(12):5340–62. 2012.

[16] Lignarolo LEM, Mehta D, Stevens RJAM, Yilmaz AE, van Kuik G, Andersen SJ, et al., R Validation of four LES and a vortex model against stereo-PIV measurements in the near wake of an actuator disc and a wind turbine, Renewable Energy, 94:510–23., 2016.

[17] Tennekes H., Lumley JL., A first course in turbulence The MIT Press, 1972.